# *Circular zymogens of human ribonuclease 1*

Raines Ronald (Orcid ID: 0000-0001-7164-1719)





# Circular Zymogens of Human Ribonuclease 1

Ian W. Windsor,[1,3] Crystal J. Graff,[1] and Ronald T. Raines[1–3]*

[1]Department of Biochemistry and [2]Department of Chemistry, University of Wisconsin−Madison, Madison, Wisconsin 53706, USA
[3]Department of Chemistry, Massachusetts Institute of Technology, Cambridge, Massachusetts 02139, USA

Additional Supporting Information may be found in the online version of this article.

Grant sponsor: NIH R01 GM008349; NIH R01 CA073808; NIH T32 GM008349.

*Correspondence to: Ronald T. Raines, Department of Chemistry, Massachusetts Institute of Technology, 77 Massachusetts Avenue, Cambridge, MA 02139, United States. E-mail: rtraines@mit.edu

**Abstract**

The endogenous production of enzymes as zymogens provides a means to control catalytic activities. Here, we describe the heterologous production of ribonuclease 1 (RNase 1), which is the most prevalent secretory ribonuclease in humans, as a zymogen. In folded RNase 1, the N and C termini flank the enzymic active site. By using intein-mediated cis-splicing, we created circular proteins in which access to the active site of RNase 1 is obstructed by an amino-acid sequence that is recognized by the HIV-1 protease. Installing a sequence that does not perturb the RNase 1 fold led to only modest inactivation. In contrast, the ancillary truncation of residues from each terminus led to a substantial decrease in the catalytic activity of the zymogen with the maintenance of thermostability. For optimized zymogens, activation by HIV-1 protease led to a $>10^4$-fold increase in ribonucleolytic activity at a rate comparable to that for the cleavage of endogenous viral substrates. Molecular modeling indicated that these zymogens are inactivated by conformational distortion in addition to substrate occlusion. Because protease levels are elevated in many disease states and ribonucleolytic activity can be cytotoxic, RNase 1 zymogens have potential as generalizable prodrugs.

Keywords: circular protein; cytotoxin; HIV; intein; protease; ribonuclease; zymogen

Abbreviations: HIV, human immunodeficiency virus; PBS, phosphate-buffered saline; RNase, ribonuclease; SDS–PAGE, polyacrylamide gel electrophoresis performed in the presence of sodium dodecyl sulfate

## INTRODUCTION

The production of a cytotoxic enzyme demands precise regulation by the host organism. Typically, safeguards attenuate enzymatic activity until its manifestation is necessary. For example, ribonucleolytic activity is controlled beneficially by endogenous ribonuclease-inhibitor proteins;[1,2] likewise, proteolytic activity is controlled by protease-inhibitor proteins.[3,4]

Another strategy has evolved to regulate catalysis by proteases. The apoptotic caspases and many other proteases are expressed as zymogens—inactive precursors that require subsequent proteolysis to mature into an active form. We and others have recognized that zymogens provide a conceptual framework for the engineering of otherwise cytotoxic enzymes as biologic "prodrugs" that are activated by pathogenic proteases. The potential of this concept was demonstrated by altering a natural zymogen, caspase 3, for activation by HIV-1 protease.[5] The first zymogen to be created *de novo* was a circularly permuted variant of ribonuclease (RNase) A in which the native N- and C-termini were connected with a linker containing the sequence recognized by the plasmepsin II protease.[6] Iterations of this strategy produced RNase A zymogens activated by the NS3 protease and HIV-1 protease.[7,8] In these RNase A zymogens, the linker occludes the active site, leading to the suppression of enzymatic activity by up to $10^3$-fold, depending on the design parameters and nature of the activating protease. The circular permutation strategy was replicated in an amphibian homologue of RNase A, though the suppression of catalytic activity was modest.[9]

Conformational distortion has also been employed in zymogen designs. Ozawa and coworkers created circular variants of firefly luciferase using intein-mediated cis-splicing to connect the termini with a caspase 3 substrate.[10] The ensuing zymogen can serve as a luminescent probe for cellular apoptosis, but exhibits a <10-fold change in signal. Later, Loh and coworkers employed structural strain to inactivate a bacterial ribonuclease, but their proteins folded properly only at low temperatures.[11]

Here, we use intein-mediated cis-splicing to create a circular variant of RNase 1 (EC 3.1.27.5; UniProtKB P07998), which is the human homolog of RNase A. By optimizing a short linker that occludes the active site, we show that conformational distortion leads to unprecedented inactivation. The optimized zymogen gains $>10^4$-fold in ribonucleolytic activity upon linker-cleavage by HIV-1 protease.

## RESULTS

### *Encoding a circular zymogen*

Circular RNase 1 zymogens were created by intein-mediated cis-splicing with the *Nostoc punctiforme* (Npu) DnaE split intein.[12] The Npu intein utilizes a "CFN" N-terminal splice junction.[13] We utilized the "CFQ" sequence that begins at residue 58 of human RNase 1. We also omitted the 4-residue C-terminal extension (residues 125–128) of RNase 1, which is not important for ribonucleolytic activity and is absent from RNase A.[14]

***Design and assessment of the glycine (G) series of zymogens***

Previous RNase A zymogens exhibited modest inactivation, suggesting that a 14-residue linker would not block the active site of RNase 1 effectively. We designed a series of zymogens to test this hypothesis by bringing the linker closer to the active site with progressively shorter linkers. Additionally, we employed a substrate identified by phage display that is cleaved efficiently by HIV-1 protease (SGIFLETS).[15] We flanked this sequence with varying numbers of glycine residues to create the G series of zymogens (Table I). A plasmid encoding the intein fragments flanking a circularly permuted RNase 1 connected by the substrate linker directed the expression of the two soluble proteins and another insoluble one corresponding to the intein fragments and the circular RNase 1 (Fig. S1), indicative of intein-mediated cyclization.[12] These zymogens all exhibited roughly two orders-of-magnitude less catalytic activity than did wild-type RNase 1, and no trend in inactivation was apparent, despite a progressive reduction in thermostability (Table SI; Fig. 1).

***Design and assessment of the strained (Str) series of zymogens***

Next, we sought to remove residues from the termini of RNase 1 with the intent of imposing strain that leads to conformational distortion. Previous crystallization studies of RNase 1 revealed that the first 7 N-terminal residues can be removed with only an order of magnitude loss in catalytic activity.[16] Lys7 is important for binding the phosphoryl group of the RNA backbone in the $P_2$ subsite.[17,18] Folding studies of RNase A demonstrated that residues beyond

122 can be removed without diminishing catalytic activity or conformational stability.[19] Hence, we excluded residues 7 through 122 from truncation. The terminal residues of our protease substrate are both serine. Removal of the three N-terminal (ΔKES) and two C-terminal (ΔSV) residues and connecting the resulting termini with the substrate sequence would replace the truncated serine residues. This construct was selected as a starting point for the strained (Str) series of zymogens and was truncated further by progressively removing residues 4, 5, and 6 (Table I). The Str1 zymogen showed a similar, two orders-of-magnitude reduction in the catalytic activity of that in the glycine series (Table SI). Further truncations reduced the catalytic activity of the zymogens substantially, with only a small reduction in thermostability (Fig. 1).

***Assessing zymogen activation by HIV-1 protease***

The zymogens that exhibited substantial inactivation, *i.e.*, $k_{cat}/K_M < 10^4$ $M^{-1}s^{-1}$, were subjected to activation studies with HIV-1 protease. Importantly, proteolysis by the protease must be limited to the inactivating linker of the zymogen. We determined that wild-type RNase 1 is not cleaved by HIV-1 protease (Fig. S2). Next, we digested zymogens with HIV-1 protease and measured the resulting ribonucleolytic activity. Proteolysis restored nearly wild-type catalytic activity to the Str2, Str3, and Str4 zymogens (Table II). Finally, we developed a continuous assay to measure the $k_{cat}/K_M$ value for HIV-1 protease cleavage of the zymogens, and found values of $k_{cat}/K_M$ between $1 \times 10^3$ $M^{-1}s^{-1}$ and $4 \times 10^3$ $M^{-1}s^{-1}$ (Tables II, SII; Fig. S3).

***Modeling the structural basis of Str2 zymogen inactivation***

The zymogen Str2 possessed the best combination of key attributes: catalytic inactivation, thermostability, and proteolytic activation. Accordingly, we modeled the Str2 zymogen with Rosetta software to reveal the structural origins of catalytic inactivation in our zymogen design. We examined the top-ten scoring models of four-hundred. In each model, we found that the N-terminal α-helix was nearly intact whereas the C-terminal β-strand adopted a distorted conformation [Fig. 2(B), S4(A)].

***Modeling the structural basis for proteolytic activation of Str2 by HIV-1 protease***

Again, we used modeling with Rosetta software to reveal the structural basis of recognition of the inactivating linker by HIV-1 protease. We examined the top-ten scoring models of two-hundred and found that the N-terminal α-helix and C-terminal β-strand must unfold completely to accommodate HIV-1 protease with its flaps closed upon a substrate sequence installed in the linker region [Fig. 2(C), S4(B)].

**DISCUSSION**

The mechanism of our zymogen inactivation relies on two key strategies: steric occlusion and conformational distortion. Roughly two orders-of-magnitude in catalytic activity are lost by installing a linker across the active site, as observed with previous circularly permuted RNase A zymogens. We suspect that this value is the limit of inactivation imposed by blocking the active

site with a flexible linker. Further inactivation was achieved through the localized installation of strain, which violated the design criteria of the previous circularly permuted zymogens[6] but was enabled herein by intein-mediated cyclization. Key active-site residues, His12 and His119, are located near the termini in an α-helix and β-strand that are not stabilized by disulfide bonds, unlike the core structure (Fig. 2). Through conformational distortion by progressive truncation, we were able to perturb the location of these active-site residues so as to achieve unprecedented level of activation of a *de novo* engineered zymogen without a prohibitive compromise to global conformational stability. For example, the circular Str2 zymogen of RNase 1 has $T_m$ = 48°C and gains 11,000-fold in catalytic efficiency upon activation with HIV-1 protease (Table 1). In contrast, the circular permutation of RNase A led to a zymogen with $T_m$ = 46°C and only a 48-fold gain in catalytic efficiency.[8] (Here, $T_m$ refers to the temperature at the midpoint of the thermal transition from the native state to denatured states.)

Our structural modeling revealed how steric occlusion and conformational distortion are operational in our zymogen design. The top-10 scoring structures are predicted to be similar in energy, yet conformationally divergent in the linker. This dichotomy suggests that the zymogen linker has a dynamic conformation, but also demonstrates unambiguously that both termini cannot adopt the wild-type fold simultaneously.

Despite the greater proximity of our linker to the active site compared to that of previous zymogens, our designs maintained efficient activation by the designated protease. We observed two-orders-of-magnitude reduction of the second-order rate constant of HIV-1 protease toward

the zymogens with respect to a fluorogenic peptide substrate, which is cleaved with a $k_{cat}/K_M$ value of $5.0 \times 10^5$ $M^{-1}s^{-1}$.[20] Our chosen substrate is, however, the sequence hydrolyzed most efficiently by HIV-1 protease. The catalytic activity of HIV-1 protease for activation of the zymogens is comparable to that for the cleavage of endogenous substrates.[21] As indicated by our modeling, the loss in catalytic efficiency results from the energetic cost of unfolding the N- and C-terminal structural elements of the zymogen to accommodate the flaps of the protease. Not all proteases employ flaps, and zymogens might be activated even more efficiently by other pathogenic proteases. For example, plasmepsins have an open active-site cleft.[22]

Ribonucleases are a privileged class of enzymes for the creation of zymogens due to attributes that are desirable for a clinical context: cell permeability and cytotoxic activity.[23] Moreover, the reliance of a chemotherapeutic agent on the activity of an enzyme (such as HIV-1 protease), rather than its inhibition, obviates common mechanisms of resistance. We anticipate, however, that translation of these results into a biomedical context could require installing residues that increase thermostability[24] and enable evasion of the cytosolic ribonuclease-inhibitor protein,[1,23,25,26] ensuring that the linker between the N and C termini is not a substrate for human proteases, and enhancing cytosolic uptake by esterification of protein carboxyl groups.[27] Efforts towards these goals are on-going in our laboratory.

## EXPERIMENTAL PROCEDURES

### *Conditions*

All procedures were performed in air at ambient temperature (22°C) and pressure (1.0 atm) unless indicated otherwise.

### *Protein expression and purification*

The RNase 1 gene was obtained as reported previously.[24] The NpuN and NpuC intein fragments were obtained from vectors provided by Tom W. Muir (Princeton University).[28] DNA oligonucleotides were obtained from Integrated DNA Technologies (Coralville, IA).

The circular RNase 1 zymogen construct was prepared initially using the linker sequence from a circularly permuted RNase A zymogen containing the p2/NC cleavage site. PCR was used to prepare five DNA fragments with terminal homology: the pET32b plasmid, NpuC, a C-terminal RNase 1 fragment, an N-terminal RNase 1 fragment, and the NpuN fragment. Gibson assembly[29] was used to combine fragments into the final expression constructs. Modification of the original plasmid was done by producing RNase 1 fragments with PCR by including the new linkers and truncations, and combining these fragments with a plasmid fragment that contained both intein fragments.

Ribonucleases were produced by heterologous expression in *Escherichia coli* and purified as previously.[24] All chromatography and assay buffers were treated with DEPC prior to use, with the exception of Tris, which was added from ribonuclease-free stocks from Invitrogen (Carlsbad,

CA). Zymogens were folded in the presence of arginine–HCl (0.5 M) and were purified with additional chromatography on a MonoS column from GE Healthcare (Chicago, IL) to ensure purity and removal of contaminating ribonucleases. HIV-1 protease was produced by heterologous expression in *E. coli* and purified as described previously.[20] Protein purity was confirmed by SDS–PAGE, and concentrations were determined by using the Pierce™ BCA assay kit from ThermoFischer Scientific (Waltham, MA). HIV-1 protease was also treated with DTT (10 mM) at 4°C for 4 h to inactivate any contaminating ribonucleases. The ensuing solution was desalted by passage through a HiTrap® Sephadex G-25 column from GE Healthcare, and did not exhibit detectable ribonucleolytic activity.

***Enzymatic activity assays***

The rate of RNA hydrolysis was monitored by the increase in fluorescence intensity of a doubly labeled fluorogenic substrate, 6-FAM–dArUdAdA–6-TAMRA, upon exposure to RNase 1 zymogens.[30] Initial ($I_o$) and final ($I_f$) intensities along with linear slopes ($\Delta I/\Delta t$) or the second derivative of quadratic fits ($2a = \Delta^2 I/\Delta t^2$) were measured and used to calculate the value of $k_{cat}/K_M$. Assays required enzyme concentrations of 10 pM–1 μM to achieve velocities that reached 10% RNA turnover within several minutes. Activated zymogens were prepared for kinetic testing by digesting the zymogen (50 μM) with HIV-1 protease (52 nM) at 37°C. Continuous activation assays were performed with a lower concentration of HIV-1 protease (2.6 nM). Fluorescence intensity was measured with a M1000 microplate reader from Tecan

(Männedorf, Switzerland) by monitoring emission at 515 nm with excitation at 493 nm. Assays were performed in quadruplicate in a flat, black 96-well plate from Corning (Corning, NY). Assay buffers were DEPC-treated and consisted of either 50 mM Tris–HCl buffer, pH 7.4, containing NaCl (100 mM) or 50 mM sodium acetate buffer, pH 5.0, containing NaCl (100 mM). Ribonucleolytic activity was assessed with eq 1 by assaying initial velocities under second-order conditions.

$$\frac{k_{\mathrm{cat}}}{K_{\mathrm{M}}} = \frac{\frac{\Delta I}{\Delta t}}{[\mathrm{ribonuclease}](I_{\mathrm{f}} - I_{\mathrm{o}})} \quad (1)$$

Steady-state kinetic parameters for zymogen cleavage by HIV-1 protease were determined with eq 2 by assaying the increase in ribonucleolytic activity observed upon the addition of the protease.

$$\frac{k_{\mathrm{cat}}}{K_{\mathrm{M}}}_{\mathrm{HIV-1\ protease}} = \frac{\frac{\Delta^2 I}{\Delta t^2}}{\left(\frac{k_{\mathrm{cat}}}{K_{\mathrm{M}}}_{\mathrm{zymogen,activated}} - \frac{k_{\mathrm{cat}}}{K_{\mathrm{M}}}_{\mathrm{zymogen,inactivated}}\right)[\mathrm{zymogen}][\mathrm{HIV-1\ protease}](I_{\mathrm{f}} - I_{\mathrm{o}})} \quad (2)$$

Values of $k_{\mathrm{cat}}/K_{\mathrm{M}}$ at pH 7.4, which is the pH optimum of RNase 1,[31] are reported in the main text. These values were also determined at pH 5.0 (Table SII), which is optimal for catalysis by HIV-1 protease, and used as parameters in the fitting of eq 2. Values of $k_{\mathrm{cat}}/K_{\mathrm{M}}$ are reported as the mean ± SD of quadruplicate measurements.

***Thermostability assays***

The thermostability of ribonucleases was determined by differential scanning fluorometry.[32] The thermostability of the G series of zymogens was determined with a CFX connect RT-PCR machine from Bio-Rad (Hercules, CA). Samples of protein (5 µM) in 25 µL of phosphate-buffered saline (PBS), pH 7.4, containing SYPRO Orange (1% v/v) (Sigma–Aldrich) were heated from 25–95°C at 1°C/min. Single fluorescent measurements per degree were recorded, and the change in fluorescence per °C was calculated with Excel software from Microsoft (Redmond, WA) by using the equation: $\Delta F_t = F_{t+1} - F_{t-1}$. The maximal change in fluorescence and the five flanking measurements above and below were fitted with the Gaussian function built into Prism 6 software from GraphPad (San Diego, CA). Values of $T_m$ are reported as the mean ± SD of triplicate measurements.

The thermostability of Str zymogens was determined with a ViiA 7 RT PCR machine from Applied Biosystems (Foster City, CA). Samples of zymogen (30 µg) in 20 µL of PBS, pH 7.4, containing SYPRO Orange (0.6% v/v) were heated from 20–96°C at 1°C/min in steps of 1°C. The value of $T_m$ was determined with Protein Thermal Shift software from Applied Biosystems using the Boltzmann model and reported as the mean ± SD of quadruplicate measurements.

***Molecular modeling***

Modeling of the Str2 zymogen and its complex with HIV-1 protease were conducted with Rosetta software.[33] RNase 1 from PDB entry 1z7x was extracted from chain A.[25] To accommodate the need for N and C termini, the structure of RNase 1 was circularly permuted by creating new termini at residues 88 and 89 while installing a linker between the original termini.[6] The 15 N-terminal and 12 C-terminal residues were removed so as to be predicted computationally. KIC loop modeling was performed using fragments picked by the Robetta Server to prepare 400 models of the zymogen linker and proximal residues of the native termini.[34,35]

Modeling of the complex was conducted in two steps. RosettaDock was employed to dock HIV-1 protease in the closed conformation bound to the "SGIFLETS" from chain A of PDB entry 6bra into the active-site cleft of the N- and C-terminally truncated structure of RNase 1.[36,37] Docking models were inspected manually to identify orientations with proximal termini of RNase 1 and the substrate in the active site of HIV-1 protease. Five docking models compatible with a zymogen·protease complex were subjected to further modeling of their loop. The docking model that generated the lowest-energy complex by loop modeling was used to prepare an additional 200 models.

The top-10 scoring models (Table SIII) are shown in Figure S4. Coordinates of these models are included in supplemental files: "Str2_top10.pdb" and "Complex_top10.pdb".

**Acknowledgments**

We thank Professor Tom W. Muir (Princeton University) for providing DNA encoding the Npu DnaE intein fragments. We are grateful to Professor Jens Meiler and Dr. Rocco Moretti (Vanderbilt University) for training and advice on the use of Rosetta software.

**Conflict of interest**

The authors declare that they have no conflicts of interest.

**REFERENCES**


1. Dickson KA, Haigis MC, Raines RT (2005) Ribonuclease inhibitor: Structure and function. Prog Nucleic Acid Res Mol Biol 80:349-374.
2. Ulyanova V, Vershinina V, Ilinskaya O (2011) Barnase and binase: Twins with distinct fates. FEBS J 278:3633-3643.
3. Ekert PG, Silke J, Vaux DL (1999) Caspase inhibitors. Cell Death Differ 6:1081-1086.
4. Huntington JA (2011) Serpin structure, function and dysfunction. J Thromb Haemost 9:26-34.
5. Vocero-Akbani AM, Heyden NV, Lissy NA, Ratner L, Dowdy SF (1999) Killing HIV-infected cells by transduction with an HIV protease-activated caspase-3 protein. Nat Med 5:29-33.
6. Plainkum P, Fuchs SM, Wiyakrutta S, Raines RT (2003) Creation of a zymogen. Nat Struct Biol 10:115-119.
7. Johnson RJ, Lin SR, Raines RT (2006) A ribonuclease zymogen activated by the NS3 protease of the hepatitis C virus. FEBS J 273:5457-5465.
8. Turcotte RF, Raines RT (2008) Design and characterization of an HIV-specific ribonuclease zymogen. AIDS Res Hum Retroviruses 24:1357-1363.
9. Callis M, Serrano S, Benito A, Laurents DV, Vilanova M, Bruix M, Ribo M (2013) Towards tricking a pathogen's protease into fighting infection: The 3D structure of a stable circularly permuted onconase variant cleavedby HIV-1 protease. PLoS One 8:e54568.

10. Kanno A, Yamanaka Y, Hirano H, Umezawa Y, Ozawa T (2007) Cyclic luciferase for real-time sensing of caspase-3 activities in living mammals. Angew Chem Int Ed 46:7595-7599.
11. Butler JS, Mitrea DM, Mitrousis G, Cingolani G, Loh SN (2009) Structural and thermodynamic analysis of a conformationally strained circular permutant of barnase. Biochemistry 48:3497-3507.
12. Evans TC, Jr., Martin D, Kolly R, Panne D, Sun L, Ghosh I, Chen L, Benner J, Liu XQ, Xu MQ (2000) Protein trans-splicing and cyclization by a naturally split intein from the dnaE gene of *Synechocystis* species PCC6803. J Biol Chem 275:9091-9094.
13. Zettler J, Schutz V, Mootz HD (2009) The naturally split *Npu* DnaE intein exhibits an extraordinarily high rate in the protein trans-splicing reaction. FEBS Lett 583:909-914.
14. Bal HP, Batra JK (1997) Human pancreatic ribonuclease—deletion of the carboxyl-terminal EDST extension enhances ribonuclease activity and thermostability. Eur J Biochem 245:465-469.
15. Beck ZQ, Hervio L, Dawson PE, Elder JH, Madison EL (2000) Identification of efficiently cleaved substrates for HIV-1 protease using a phage display library and use in inhibitor development. Virology 274:391-401.
16. Pous J, Mallorqui-Fernandez G, Peracaula R, Terzyan SS, Futami J, Tada H, Yamada H, Seno M, de Llorens R, Gomis-Ruth FX, Coll M (2001) Three-dimensional structure of human RNase 1 delta N7 at 1.9 Å resolution. Acta Cryst D57:498-505.

17. Fontecilla-Camps JC, de Llorens R, le Du MH, Cuchillo CM (1994) Crystal structure of ribonuclease A.d(ApTpApApG) complex. Direct evidence for extended substrate recognition. J Biol Chem 269:21526-21531.
18. Fisher BM, Ha JH, Raines RT (1998) Coulombic forces in protein–RNA interactions: Binding and cleavage by ribonuclease A and variants at Lys7, Arg10, and Lys66. Biochemistry 37:12121-12132.
19. Fujii T, Ueno H, Hayashi R (2002) Significance of the four carboxyl terminal amino acid residues of bovine pancreatic ribonuclease A for structural folding. J Biochem 131:193-200.
20. Windsor IW, Raines RT (2015) Fluorogenic assay for inhibitors of HIV-1 protease with sub-picomolar affinity. Sci Rep 5:11286.
21. Tozser J, Blaha I, Copeland TD, Wondrak EM, Oroszlan S (1991) Comparison of the HIV-1 and HIV-2 proteinases using oligopeptide substrates representing cleavage sites in Gag and Gag-Pol polyproteins. FEBS Lett 281:77-80.
22. Silva AM, Lee AY, Gulnik SV, Maier P, Collins J, Bhat TN, Collins PJ, Cachau RE, Luker KE, Gluzman IY, Francis SE, Oksman A, Goldberg DE, Erickson JW (1996) Structure and inhibition of plasmepsin II, a hemoglobin-degrading enzyme from *Plasmodium falciparum*. Proc Natl Acad Sci USA 93:10034-10039.
23. Lomax JE, Eller CH, Raines RT (2012) Rational design and evaluation of mammalian ribonuclease cytotoxins. Methods Enzymol 502:273-290.

24. Leland PA, Staniszewski KE, Kim BM, Raines RT (2001) Endowing human pancreatic ribonuclease with toxicity for cancer cells. J Biol Chem 276:43095-43102.

25. Johnson RJ, McCoy JG, Bingman CA, Phillips GN, Jr., Raines RT (2007) Inhibition of human pancreatic ribonuclease by the human ribonuclease inhibitor protein. J Mol Biol 368:434-449.

26. Rutkoski TJ, Raines RT (2008) Evasion of ribonuclease inhibitor as a determinant of ribonuclease cytotoxicity. Curr Pharm Biotechnol 9:185-199.

27. Ressler VT, Mix KA, Raines RT (2019) Esterification delivers a functional enzyme into a human cell. ACS Chem Biol 14:599-602.

28. Shah NH, Vila-Perello M, Muir TW (2011) Kinetic control of one-pot trans-splicing reactions by using a wild-type and designed split intein. Angew Chem Int Ed 50:6511-6515.

29. Gibson DG, Young L, Chuang R-Y, Venter JC, Hutchison CA, III, Smith HO (2009) Enzymatic assembly of DNA molecules up to several hundred kilobases. Nat Methods 6:343-345.

30. Kelemen BR, Klink TA, Behlke MA, Eubanks SR, Leland PA, Raines RT (1999) Hypersensitive substrate for ribonucleases. Nucleic Acids Res 27:3696-3701.

31. Eller CH, Lomax JE, Raines RT (2014) Bovine brain ribonuclease is the functional homolog of human ribonuclease 1. J Biol Chem 289:25996-26006.

32. Senisterra G, Chau I, Vedadi M (2012) Thermal denaturation assays in chemical biology. Assay Drug Dev Technol 10:128-136.

33. O'Meara MJ, Leaver-Fay A, Tyka MD, Stein A, Houlihan K, DiMaio F, Bradley P, Kortemme T, Baker D, Snoeyink J, Kuhlman B (2015) Combined covalent-electrostatic model of hydrogen bonding improves structure prediction with Rosetta. J Chem Theory Comput 11:609-622.
34. Gront D, Kulp DW, Vernon RM, Strauss CE, Baker D (2011) Generalized fragment picking in Rosetta: Design, protocols and applications. PLoS One 6:e23294.
35. Stein A, Kortemme T (2013) Improvements to robotics-inspired conformational sampling in Rosetta. PLoS One 8:e63090.
36. Wang C, Bradley P, Baker D (2007) Protein–protein docking with backbone flexibility. J Mol Biol 373:503-519.
37. Windsor IW, Raines RT (2018) A substrate selected by phage display exhibits enhanced side-chain hydrogen bonding to HIV-1 protease. Acta Cryst D74:690-694.

**Table I.** *Amino-acid Sequences of RNase 1 Zymogens*

| Zymogen | Linker | N-truncation | C-truncation |
|---|---|---|---|
| 3G | GGGSGIFLETSGGG | None | EDST |
| 2G | GGSGIFLETSGG | None | EDST |
| 1G | GSGIFLETSG | None | EDST |
| 0G | SGIFLETS | None | EDST |
| Str1 | SGIFLETS | KES | SVEDST |
| Str2 | SGIFLETS | KESR | SVEDST |
| Str3 | SGIFLETS | KESRA | SVEDST |
| Str4 | SGIFLETS | KESRAK | SVEDST |

**Table II.** *Properties of Three RNase 1 Zymogens*

| Zymogen | $k_{cat}/K_M$ ($M^{-1}s^{-1}$)[a] (inactive) | $k_{cat}/K_M$ ($M^{-1}s^{-1}$)[a] (activated) | Relative Activity[a] | $k_{cat}/K_M$ ($M^{-1}s^{-1}$)[b] (HIV-1 protease) | $T_m$[a] (°C) |
|---|---|---|---|---|---|
| Str2 | $(5.8 \pm 0.2) \times 10^3$ | $(6.7 \pm 0.1) \times 10^7$ | 11,000 | $(3.9 \pm 0.3) \times 10^3$ | $47.5 \pm 0.1$ |
| Str3 | $(1.1 \pm 0.1) \times 10^3$ | $(3.2 \pm 0.1) \times 10^6$ | 2,800 | $(1.3 \pm 0.1) \times 10^3$ | $42.6 \pm 0.1$ |
| Str4 | $(5.7 \pm 0.1) \times 10^2$ | $(1.4 \pm 0.1) \times 10^7$ | 24,000 | $(2.5 \pm 0.1) \times 10^3$ | $42.0 \pm 0.1$ |

[a]Assays were performed at pH 7.4.
[b]Assays were performed at pH 5.0.

**Figure Legends**

**Figure 1.** Graph of the catalytic efficiency ($k_{cat}/K_M$, log scale) and thermostability ($T_m$, linear scale) of circular zymogens of RNase 1. Values are the mean ± SD. Values for RNase 1 are from ref. [25].

**Figure 2.** Ribbon diagrams of the structure of RNase 1, the Str2 zymogen, and its complex with HIV-1 protease. The side chains of key active-site residues (His12, Lys41, and His119 of RNase 1; Asp25 of HIV-1 protease) and cystine residues are shown explicitly. (A) Crystal structure of RNase 1 (PDB entry 1z7x, chain A). (B) Model of the structure of the Str2 zymogen as predicted with Rosetta software. Four residues are truncated from the N terminus and 6 residues from the C terminus of RNase 1, and the resulting termini are connected with a linker (green). To accommodate the software, new termini are generated at residues 88 and 89. (C) Model of the structure of the complex of the Str2 zymogen and HIV-1 protease as predicted with Rosetta software.

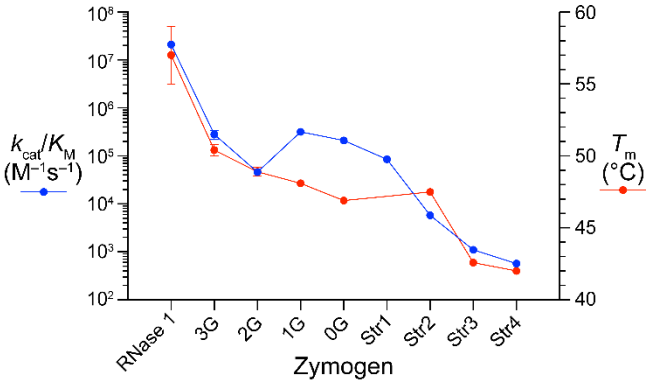

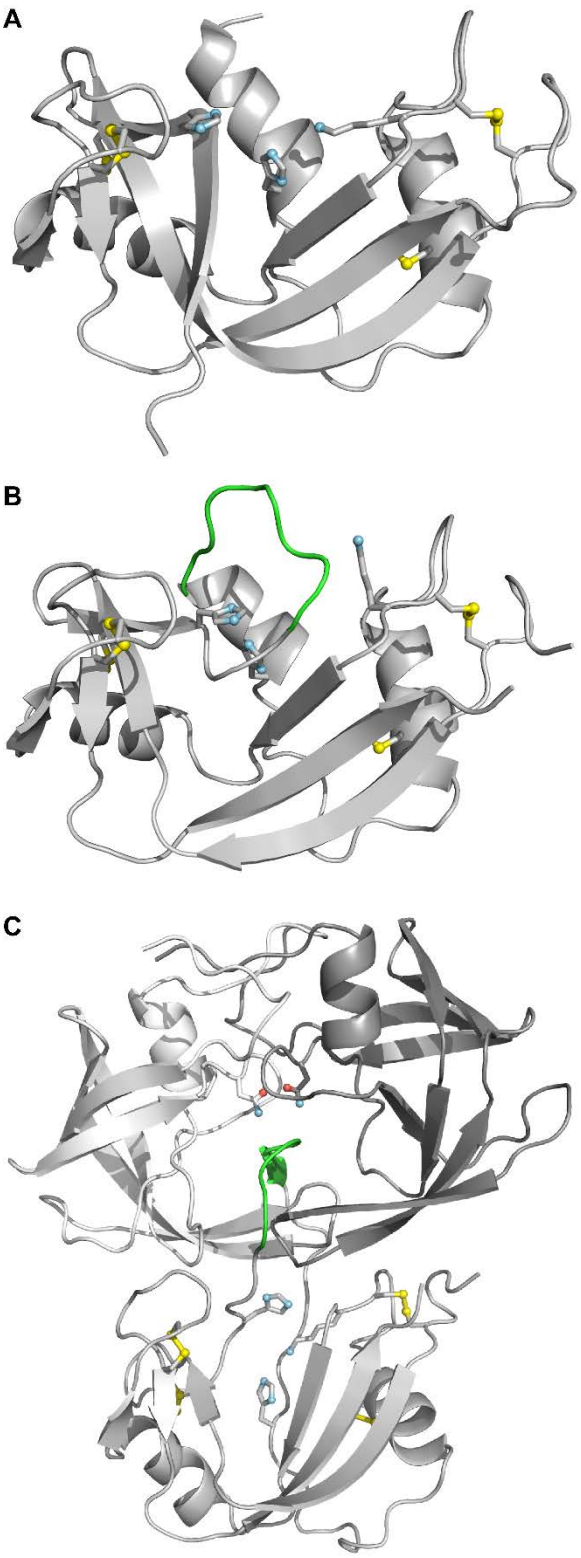

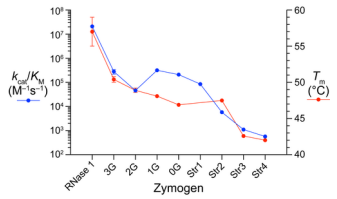


PRO_3686_Figure_1.tif

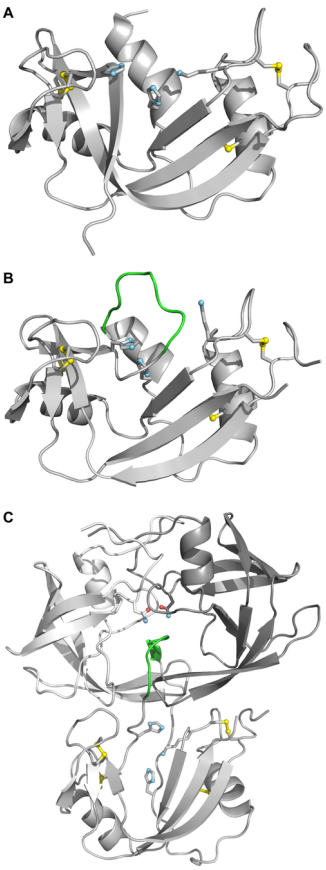


PRO_3686_Figure_2.tif